The Deep Flow through the Northeast Channel, Gulf of Maine†

STEVEN R. RAMP, RONALD J. SCHLITZ AND W. REDWOOD WRIGHT*

National Marine Fisheries Service, Northeast Fisheries Center, Woods Hole, MA 02543

(Manuscript received 4 October 1982, in final form 27 June 1985)

ABSTRACT

The flow dynamics, volume, heat, and nitrogen transport, and water mass structure in the Northeast Channel (42°17'N, 65°58'W) are investigated using two years of moored velocity and temperature data. Measurements were made from September 1976 to September 1978 at three moorings across the channel just inside the sill with instruments at 100 m, 150 m, and 16 m off the bottom. Energetic water motions occurred at three time scales: 1) tidal frequencies; 2) low-frequency motions in the 4–10-day range; and 3) mean motions with periods of three months or longer. The dominant tidal constituent was the semidiurnal (M_2) tide, whose elipses all rotated clockwise, with magnitudes ranging from 61 cm s^{-1} at 150 m depth decreasing to 41 cm s^{-1} 16 m off the bottom. The low-frequency currents showed strong seasonal variability: In winter, these motions took the form of strong bursts of current up to 50 cm s^{-1} both into and out of the channel, and were the dominant subtidal motions; in summer, these bursts were small and were superimposed on a steady inflow (northeast side) or outflow (southwest side). The low-frequency currents were strongly correlated with surface wind stress and coastal synthetic subsurface pressure (SSP), suggesting that outflows and inflows in the 4–10-day range were associated with a large-scale setup or setdown of the Gulf of Maine by the wind stress. The mean currents were partitioned year-round into an inflow and an outflow region. Outflows occurred at 100 m and 150 m depth on the southwest side of the channel with mean magnitudes of 7 and 2 cm s^{-1}, respectively. Inflows occurred everywhere else, with magnitudes of about 10 cm s^{-1} at 100 m decreasing to about 3 cm s^{-1} toward the bottom.

The total integrated volume transport below 75 m depth at two week intervals was highly variable, but when averaged over the entire dataset, it was in-channel at a rate of 262 ± 58 ($\times 10^3$ m^2 s^{-1}), which gave a replacement time of about 11 ± 2 months for deep waters of the Gulf of Maine. The temperature time series suggested that the inflowing water consisted of both Warm Slope Water (WSW) and Labrador Slope Water (LSW). The eddy heat flux added heat to the deep waters of the Gulf of Maine at a rate of 173 × 10^6 kcal s^{-1}. A highly simplified nitrogen transport estimate suggested that at least 4.05 × 10^9 μmol s^{-1} was advected through the channel, and possibly as much as 5.87 × 10^9 μmol s^{-1} if the NH_4 contribution was included.

1. Introduction

Two years of current measurements in the Northeast Channel below 100 m were completed in September 1978 by the Northeast Fisheries Center, NMFS/NOAA. Northeast Channel, with a sill depth of about 230 m, is the only deep passage connecting the Slope Water of the Northwest Atlantic Ocean with the basins of the Gulf of Maine. The channel, with mooring locations and surrounding bathymetry, is shown in Fig. 1 in relation to regional land masses. The purpose of the experiment was three-fold: 1) to estimate the transport of warm, high-salinity, nutrient-rich Slope Water into the Gulf of Maine through this passage, where it may ultimately be mixed upwards to the photic zone and be utilized by marine organisms; 2) to examine the important time scales over which the variability of the channel flow occurs; and 3) to examine the forcing mechanisms that drive the flow.

Previous research focused on the Northeast Channel is limited, although it is sometimes mentioned in studies of the entire Gulf of Maine region. Bigelow (1927) commented on many features of the flow in the channel. He suggested that in the deep water, inflow occurs on the northeast side of the channel, while outflow occurs on the southwest side. He also suggested that the flow occurs in distinct "pulses," has definite seasonal variability, and that large indraft events or "invasions" of Slope Water may occasionally occur through the channel. Wright (1979) documented one such event using hydrographic data. Lauzier (1967) and Bumpus (1973, 1976) both noted a divergence in the bottom flow in the channel based on results from a small number of bottom drifters. They inferred a northeastward flow on the northeast side of the channel, and southwestward drift on the southwest side; their results, however, were highly biased by the location of maximum fishing effort in the area that determined where most of the drifters were recovered. Colton (1968, 1969) demonstrated that the type of water flow-

† Contribution Number MED/NEFC 82-7 of the NMFS Marine Resources Monitoring, Assessment and Prediction (MARMAP) Program.

* Present Affiliation: Associated Scientists at Woods Hole, Inc., Woods Hole, MA 02543.

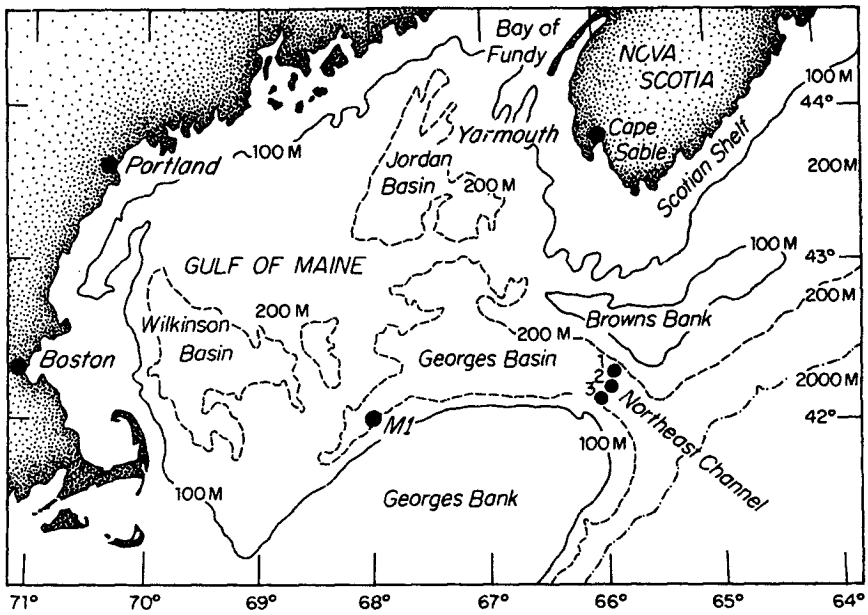

FIG. 1. The Gulf of Maine, offshore banks, and the Northeast Channel, showing bathymetry, mooring positions, and locations where coastal sea level and offshore bottom pressure measurements were made.

ing through the channel is variable, and may sometimes be "Labrador-Coastal" Water instead of Slope Water. Previous volume transport estimates for the channel have been inferred from hydrographic data rather than measured directly (Brown and Beardsley, 1978; Hopkins and Garfield, 1979).

In this paper, two years of moored current and temperature data from across the channel are used to describe the flow field in this important passage to the Gulf of Maine. Processing methods and supplementary data sources are described in Section 2. Basic results including the tidal analysis, mean flow, temperature time series, and low-frequency currents are described in Section 3, and the transport estimates are presented in Section 4. Some ideas concerning the relationship between the wind stress, the subsurface pressure field, and the currents measured in the Northeast Channel are discussed in Section 5, with the summary following in Section 6.

2. Data and methods

Nine vector-averaging current meters (VACMs) were maintained on three moorings set across the channel axis from September 1976 to September 1978. Four six-month deployments were planned, but because of logistical problems, the second deployment was delayed and a two-and-a-half-month gap exists from 21 April to 12 June 1977. The current meter moorings were deployed along a southwest–northeast line across the channel just inside the sill, with VACMs at depths of 100, 150, and 16 m off the bottom. In the following text, specific instruments are referred to using a three digit code. The first number is the deployment number (1–4), the second number is the mooring number (1–3), and the third number represents instrument depth (1 = 100 m, 2 = 150 m, 3 = 16 m off the bottom). The data are also referred to by season. The "winter" refers to mid-September through March, "spring" refers to April through May, and "summer" refers to June through mid-September.

A schematic view of the array looking into the Gulf of Maine is shown in Fig. 2 with the mooring and instrument numbers for each instrument. The data return for the experiment is included in Table 1. All instru-

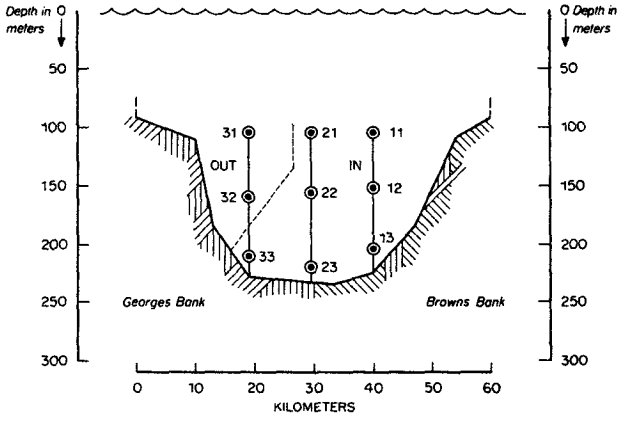

FIG. 2. Cross-sectional view of the Northeast Channel array, looking northwest into the Gulf of Maine. The first number is the mooring number and the second represents instrument depth. "IN" and "OUT" are explained in the text.

TABLE 1. Data return and basic statistics for the current data from the Northeast Channel. The mean, standard error (Std. error), low-frequency standard deviation (Lf std. dev.) and total standard deviation (Total std. dev.) are shown for each velocity component as well as the mean speed and direction, using all available data at each location.

						u (cm s^{-1})				v (cm s^{-1})					
	Instrument depth	Velocity data (days)	Temperature data (days)	Start (yr-mo)	Stop (yr-mo)	Mean	Std. error	Lf std. dev.	Total std. dev.	Mean	Std. error	Lf std. dev.	Total std. dev.	Mean speed (cm s^{-1})	Direction (deg T)
Site 1	102	555	555	76-09	77-04	0.6	0.5	5.7	15.0	10.1	1.1	11.2	31.5	10.1	3
42°22′N, 65°56.6′W				77-06	77-09										
221 m depth				77-09	77-12										
				78-03	78-09										
	152	655	655	76-09	77-04	−0.6	0.4	5.1	17.9	7.8	1.1	12.5	43.6	7.8	356
				77-06	77-09										
				77-09	78-03										
				78-03	78-09										
	204	601	601	76-09	77-04	0.3	0.3	3.9	13.5	3.3	1.2	12.8	38.1	3.3	5
				77-06	77-09										
				77-09	78-01										
				78-03	78-09										
Site 2	105	63	271	78-03	78-05	0.9				2.5				2.7	20
42°16.8′N, 65°57.0′W	155	352	665	77-09	78-03	1.4	0.8	6.7	20.7	6.2	2.3	19.1	47.4	6.4	13
232 m depth				78-03	78-09										
	216	422	448	76-09	77-04	0.5	0.4	3.8	16.7	4.5	1.7	15.8	41.0	4.5	6
				77-06	77-07										
				77-09	78-03										
Site 3	108	319	319	77-06	77-09	3.5	0.5	3.8	15.7	−6.2	0.8	6.8	45.3	7.1	150
42°10.7′N, 66°02.3′W				77-09	77-10										
229 m depth				78-03	78-09										
	158	99	282	77-06	77-09	1.6	0.6	2.7	22.3	−1.3	1.6	7.1	46.1	2.1	129
	211	372	473	77-09	78-03	1.1	0.6	4.9	17.4	9.4	2.7	22.7	41.2	9.5	7
				78-03	78-09										

ments were recovered except those on mooring 3, deployment 1. The data were processed using time-series software developed at the Woods Hole Oceanographic Institution. The original 15-minute series of east (u), north (v), speed (s), and direction (θ) were vector-averaged to hourly time series. Hourly temperature series were formed by scalar-averaging. The coordinate system was rotated counter-clockwise 48 degrees from true north so that the v component represented along-channel flow (positive in-channel) and the u component represented across-channel flow (positive northeast). For investigating wind forcing and other subtidal phenomena, the hourly records were low-passed with a digital filter having a half-power point at 33 hours (Flagg *et al.*, 1976).

Six-hourly estimates of geostrophic surface wind and wind stress vectors at 42°N, 66°W (about 18 km south of mooring 3), as calculated from large-scale pressure fields were obtained from Fleet Numerical Oceanographic Central in Monterey, California. The wind stress vectors were calculated using a constant drag coefficient $C_d = 0.0013$, and were rotated to match the coordinate system used to present the current data. Relative to the bathymetry of the continental slope, the v wind component represents cross-shore wind (positive onshore) and the u component is alongshore wind (positive northeast).

Hydrographic data were taken along the mooring line during each of the five deployment and recovery cruises. These data were supplemented with more hydrographic data taken during a cooperative sampling program in the channel from September 1975 through June 1977 (Pawlowski, 1977). Nitrogen values from the Slope Water region near the channel mouth have been obtained from two sources: historical data (1933–71) in the files of the National Oceanographic Data Center, and recent (1976–78) data from Georges Bank and vicinity reported by EG&G Environmental Consultants, Inc. (EG&G, 1978, 1979a).

3. Results

a. Tidal currents

Tides dominated the current velocity field in the Northeast Channel year-round. The tides always accounted for at least 50% of the current variance, and sometimes as much as 85% when the low-frequency events were small. The tidal analysis was conducted using the harmonic method of Dennis and Long (1971), as described by Moody *et al.* (1984). Results for the M_2, S_2, N_2, K_1, and O_1 tidal lines are shown in Table 2. The table shows that the M_2 tide was the dominant tide by far, with all other tides having a magnitude no greater than about one-fifth of the M_2 tide. Diurnal tides were small (1–3 cm s^{-1}), and made little contribution to the kinetic energy in the channel. The M_2 tidal ellipses at all the instruments were highly polarized by topography and had current vectors that rotated in a clockwise sense around the ellipse. The major axes of ellipses at 100 m depth were typically aligned with the channel axis and had a magnitude of about 50 cm s^{-1}, compared to about 20 cm s^{-1} for the minor axes. The tides had their greatest magnitudes at the 150 m depth (Table 2), possibly because of the contribution of the baroclinic (internal) tides. Toward the bottom, the magnitude of the tidal ellipses decrease by about 10 cm s^{-1} for each axis, and the entire ellipse rotated about 20° clockwise. This is apparently due to the interaction of the tidally oscillating current with the depth-averaged mean current (Tee, 1979) and is consistent with the results of Brown (1984).

b. Mean currents

The mean current vectors for each of the four deployments are shown in Fig. 3. The mean currents at moorings 1 and 2 and near the bottom at mooring 3 were directed into the Gulf of Maine with speeds ranging from 12.8 to 2.2 cm s^{-1}. The mean currents at mooring 3 at the 100 m and 150 m depths were directed out of the Gulf of Maine, at speeds ranging from 12.0 to 2.2 cm s^{-1}. Thus, there were two distinct regions of inflow and outflow to the Gulf of Maine, as shown schematically in Fig. 2. The speed decreased with depth at moorings 1 and 2, and reversed with depth at mooring 3, resulting in a strong shear zone between the 158 and 211 m depths at mooring 3. The inflow near the bottom was stronger at mooring 3 (9.4 cm s^{-1}) than at moorings 1 and 2 (3.3 and 4.5 cm s^{-1}, respectively). The best estimates of the mean speed, standard error of the mean, total standard deviation, and low-frequency standard deviation using the combined data for all four deployments are shown in Table 1.

c. Low-frequency currents and winds

The horizontal and vertical distribution of current in the channel is illustrated in Fig. 4 for the second deployment, which is typical of all four deployments. Instruments 231 and 232 (top two panels) are in the outflow region. At 231, the flow was primarily out-channel at 5–15 cm s^{-1}. At 232 (162 m), the flow was of mixed direction but the mean flow was also out of the Gulf of Maine. The bottom four panels of Fig. 4 show a steady inflow of about 20 cm s^{-1}. Like the tides, the low-frequency flow at all instruments was strongly polarized by topography, with strong axial current and little cross-channel flow. The weak cross-channel components showed no significant coherence either horizontally or vertically, indicating space scales of less than the mooring separation of 10 km. Coherence and phase calculations for the second year's data (Fig. 5) showed the axial currents in the inflow region to be highly coherent at near-zero phase lag at periods ranging from 2 to 30 days. During array 4 (Fig. 5, right half) there was a low in the coherence plots between instrument 411 and other instruments due to a spectral peak at 5

TABLE 2. Tidal current parameters for the five most significant tidal constituents in the Northeast Channel. Phases are presented relative to the Greenwich epoch (deg-G). The orientation is the angle that the major axis makes with true north (deg-True).

Station lat. long.	Record length (days)	Instrument depth (m)	Above bottom (m)	Fourier coefficients				Current ellipse parameters			
				East (cm s^{-1})	Phase (deg-G)	North (cm s^{-1})	Phase (deg-G)	Major axis (cm s^{-1})	Minor axis (cm s^{-1})	Phase (deg-G)	Orientation (deg-True)
Northeast Channel—M_2 Tide											
NEC1	174	103	120	17.0 ± 1.8	101 ± 15	51.2 ± 2.8	357 ± 4	51.4 ± 3.0	−16.1 ± 1.1	355 ± 3	335 ± 4
42°22′N	174	153	70	21.5 ± 2.7	85 ± 6	57.5 ± 3.2	355 ± 4	57.5 ± 3.2	−21.4 ± 2.7	355 ± 2	360 ± 2
65°56′W	174	207	16	16.9 ± 1.9	23 ± 15	46.2 ± 1.1	338 ± 4	47.8 ± 0.8	−11.3 ± 1.8	341 ± 3	15 ± 4
NEC2*	58	106	134	11.8 ± 1.6	99 ± 4	48.5 ± 0.0	358 ± 1	48.6 ± 0.1	−11.6 ± 1.4	358 ± 1	357 ± 2
42°18′W	174	156	84	24.4 ± 3.5	85 ± 5	56.6 ± 3.1	354 ± 2	56.6 ± 3.1	−24.3 ± 3.5	354 ± 2	360 ± 3
65°58′W	58	217	17	15.6 ± 2.7	73 ± 5	41.4 ± 12.2	346 ± 4	41.4 ± 12.2	−15.6 ± 2.7	347 ± 4	2 ± 1
NEC3*	87	112	116	16.1 ± 3.9	107 ± 2	57.8 ± 2.8	3 ± 3	57.9 ± 2.8	−15.5 ± 3.9	2 ± 3	356 ± 0
42°11′N	87	162	66	28.4 ± 1.3	72 ± 6	60.5 ± 3.1	358 ± 2	61.2 ± 2.8	−27.0 ± 1.7	3 ± 1	9 ± 2
66°02′W	174	220	16	20.5 ± 4.7	29 ± 9	47.1 ± 2.5	343 ± 3	49.5 ± 2.8	−13.9 ± 3.3	348 ± 2	18 ± 5
Northeast Channel—N_2 Tide											
NEC1	174	103	120	3.2 ± 1.3	85 ± 49	10.5 ± 1.2	331 ± 8	10.6 ± 1.1	−2.4 ± 2.0	331 ± 8	355 ± 8
42°22′N	174	153	70	4.7 ± 1.3	53 ± 27	12.1 ± 2.1	324 ± 7	12.2 ± 2.1	−4.5 ± 1.4	324 ± 5	360 ± 9
65°56′W	174	207	16	2.9 ± 2.5	357 ± 68	8.7 ± 2.0	312 ± 10	9.0 ± 1.9	−1.9 ± 2.6	314 ± 7	10 ± 13
NEC2*	58	106	134	3.8 ± 1.7	102 ± 44	9.2 ± 1.5	332 ± 5	9.4 ± 1.2	−2.9 ± 2.8	329 ± 6	348 ± 6
42°18′N	174	156	84	5.1 ± 1.4	60 ± 17	11.4 ± 1.3	327 ± 8	11.4 ± 1.3	−5.0 ± 1.5	326 ± 7	359 ± 6
65°58′W	58	217	17	4.8 ± 0.6	67 ± 52	12.6 ± 3.4	353 ± 47	12.7 ± 3.3	−4.6 ± 0.7	355 ± 45	7 ± 4
NEC3*	87	112	116	4.9 ± 0.9	100 ± 23	12.9 ± 0.1	335 ± 8	13.1 ± 0.3	−3.9 ± 1.7	331 ± 8	348 ± 3
42°11′N	87	162	66	5.4 ± 1.4	29 ± 5	11.7 ± 0.9	322 ± 5	11.9 ± 0.9	−4.7 ± 1.2	327 ± 8	12 ± 6
66°02′W	174	220	16	5.1 ± 2.4	338 ± 12	8.3 ± 1.5	309 ± 10	9.6 ± 1.9	−2.2 ± 1.5	316 ± 6	29 ± 12

Northeast Channel—S_2 Tide											
NEC1	174	103	120	2.8 ± 1.0	139 ± 18	9.2 ± 0.9	39 ± 4	9.2 ± 0.9	−2.7 ± 1.0	38 ± 3	357 ± 5
42°22′N	174	153	70	3.5 ± 1.3	118 ± 14	9.7 ± 1.3	37 ± 5	9.7 ± 1.3	−3.4 ± 1.3	37 ± 5	5 ± 4
65°56′W	174	207	16	2.6 ± 1.5	34 ± 57	6.4 ± 0.5	22 ± 6	6.8 ± 0.8	−1.2 ± 1.8	24 ± 3	13 ± 13
NEC2*	58	106	134	2.3 ± 0.5	91 ± 19	8.4 ± 0.7	34 ± 5	8.5 ± 0.8	−1.8 ± 0.1	36 ± 4	9 ± 4
42°18′N	174	156	84	3.3 ± 1.6	127 ± 22	8.9 ± 1.2	34 ± 3	8.9 ± 1.2	−3.1 ± 1.7	35 ± 2	0 ± 6
65°58′W	58	217	17	3.9 ± 2.9	62 ± 38	8.4 ± 3.6	5 ± 52	8.6 ± 3.8	−3.3 ± 2.8	10 ± 49	14 ± 2
NEC3*	87	112	116	3.1 ± 0.7	130 ± 50	10.5 ± 0.6	42 ± 8	10.6 ± 0.8	−2.6 ± 1.1	41 ± 7	358 ± 11
42°11′N	87	162	66	4.5 ± 2.2	108 ± 6	10.7 ± 2.9	40 ± 5	10.8 ± 3.0	−4.1 ± 2.2	43 ± 4	10 ± 0
66°02′W	174	220	16	2.8 ± 1.1	35 ± 27	6.4 ± 1.2	23 ± 14	6.8 ± 1.3	−0.6 ± 1.7	25 ± 9	20 ± 5
Northeast Channel—K_1 Tide											
NEC1	174	103	120	3.0 ± 0.3	19 ± 10	2.1 ± 0.6	143 ± 41	3.4 ± 0.5	+1.4 ± 0.7	194 ± 16	286 ± 27
42°22′N	174	153	70	2.0 ± 0.3	18 ± 19	2.6 ± 0.3	143 ± 14	3.1 ± 0.3	+1.4 ± 0.5	156 ± 25	330 ± 26
65°56′W	174	207	16	1.9 ± 0.3	8 ± 8	3.0 ± 0.7	134 ± 5	3.2 ± 0.7	+1.3 ± 0.2	147 ± 9	333 ± 8
NEC2*	58	106	134	3.3 ± 0.7	21 ± 14	1.8 ± 0.4	122 ± 44	3.6 ± 0.3	+1.2 ± 0.1	197 ± 26	281 ± 33
42°18′N	174	156	84	1.8 ± 0.6	44 ± 13	2.7 ± 0.6	131 ± 11	2.9 ± 0.6	+1.6 ± 0.4	118 ± 35	13 ± 37
65°58′W	58	217	17	1.6 ± 0.1	6 ± 5	2.5 ± 0.3	109 ± 23	2.6 ± 0.4	+1.4 ± 0.2	111 ± 35	353 ± 23
NEC3*	87	112	116	1.3 ± 0.4	43 ± 14	2.6 ± 0.7	146 ± 7	2.6 ± 0.7	+1.2 ± 0.5	149 ± 5	353 ± 3
42°11′N	87	162	66	0.8 ± 0.1	23 ± 10	3.0 ± 0.3	153 ± 10	3.0 ± 0.3	+0.6 ± 0.1	155 ± 10	350 ± 1
66°02′W	174	220	16	1.2 ± 0.3	352 ± 21	2.6 ± 0.3	154 ± 17	2.8 ± 0.3	+0.3 ± 0.2	157 ± 18	337 ± 7
Northeast Channel—O_1 Tide											
NEC1	174	103	120	3.0 ± 0.4	304 ± 19	1.2 ± 0.6	102 ± 87	3.3 ± 0.4	+0.2 ± 0.5	101 ± 85	322 ± 77
42°22′N	174	153	70	2.1 ± 0.8	298 ± 25	1.8 ± 0.1	58 ± 31	2.5 ± 0.4	+1.2 ± 0.5	87 ± 63	320 ± 59
65°55′W	174	207	16	2.4 ± 0.6	294 ± 18	1.8 ± 0.4	41 ± 18	2.6 ± 0.4	+1.5 ± 0.4	79 ± 63	317 ± 59
NEC2*	58	106	134	2.9 ± 1.4	302 ± 11	1.2 ± 0.2	104 ± 32	3.1 ± 1.4	+0.3 ± 0.3	118 ± 15	293 ± 5
42°18′N	174	156	84	2.0 ± 0.7	300 ± 13	1.9 ± 0.4	56 ± 13	2.4 ± 0.5	+1.3 ± 0.3	90 ± 16	313 ± 23
65°58′W	58	217	17	2.0 ± 0.1	298 ± 42	2.5 ± 0.8	21 ± 21	3.0 ± 0.8	+1.2 ± 0.0	29 ± 48	352 ± 54
NEC3*	87	112	116	0.9 ± 0.1	324 ± 9	1.2 ± 0.8	70 ± 7	1.4 ± 0.5	+0.6 ± 0.4	41 ± 41	317 ± 41
42°11′N	87	162	66	1.1 ± 0.4	270 ± 20	1.8 ± 0.4	84 ± 10	2.1 ± 0.5	+0.1 ± 0.2	86 ± 12	329 ± 7
66°02′W	174	220	16	0.8 ± 0.5	296 ± 41	1.2 ± 0.5	67 ± 38	1.4 ± 0.6	+0.3 ± 0.2	83 ± 48	328 ± 28

If Minor axis < 0, ellipse rotates clockwise.
*—Data are from two separate moorings at different times.

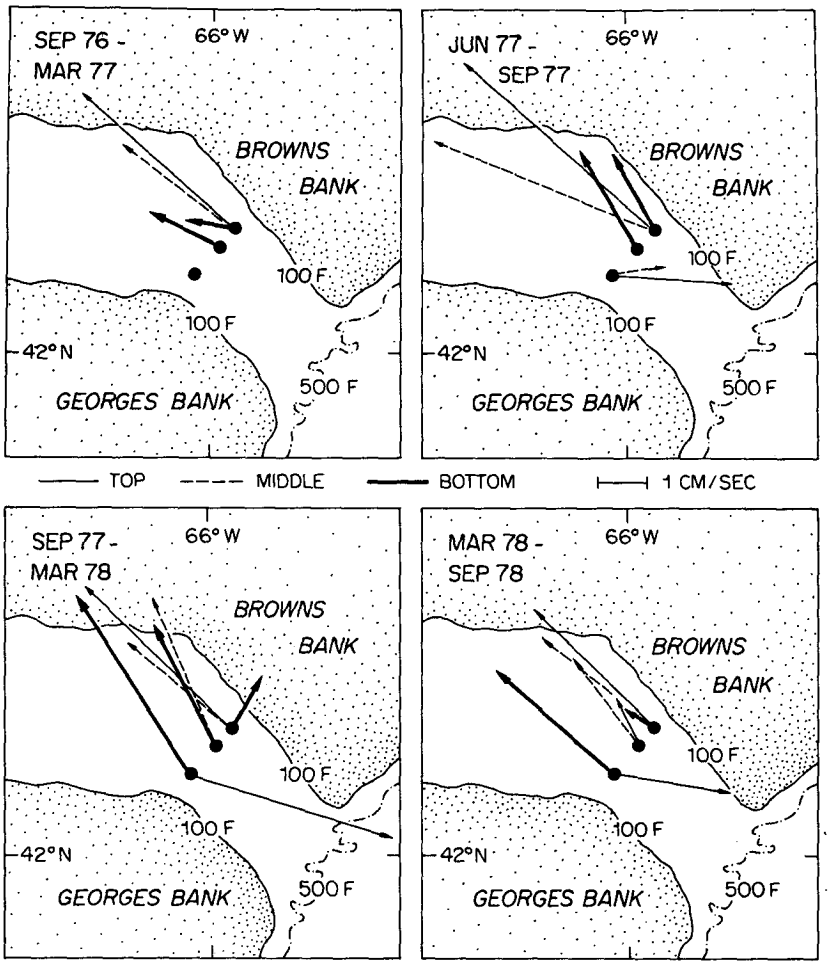

FIG. 3. Mean flow vectors in the Northeast Channel for each six-month deployment.

days at 411, which was not present at the other locations. Inadequate data return at mooring 3 precluded a rigorous analysis of the coherence and phase between the inflow and outflow regions.

The seasonal variation of the surface wind stress and current in the inflow region is shown in Fig. 6 for September 1977–September 1978. The wind measurements presented agree with earlier meteorological datasets that show that the prevailing winter winds are from the northwest, and are stronger and more variable than the prevailing summer winds from the southwest. Autospectra calculated from the wind stress (not shown) show that the winter winds were approximately three times more energetic than the spring and summer winds during the experiment. The dominant periods for the wind variability during winter (Fig. 6) ranged from 2 to 10 days. The transition to summertime southwest winds occurs at about 20 May in Fig. 6. Prior to that time, wind stress in excess of 4 dyn. cm^{-2} was common. After 20 May the wind stress rarely exceeded 0.5 dyn cm^{-2}.

The current vectors displayed in Fig. 6 also exhibit strong seasonal variation, with the changes occurring at approximately the same time as the seasonal changes in wind. These vectors are from instruments 312 and 412 and are taken as representative of currents in the inflow region because of the strong coherence previously demonstrated. From 1 October through 25 April there is strong variability in the current field at 4–11 day time scales. There are strong "bursts" of current, both into and out of the Gulf of Maine, with speeds up to 60 cm s^{-1}. The inflowing bursts occur more frequently and have greater magnitude and duration than the outflow bursts, so that the net mean flow is into the Gulf of Maine. During late spring (25 April–20 May) the currents in the Northeast Channel were still variable, but the magnitude of the bursts of current was much reduced from winter months. The summer currents then flowed steadily into the channel at about 20 cm s^{-1}.

During summer when the wind stress was quite small, there was no significant coherence between wind

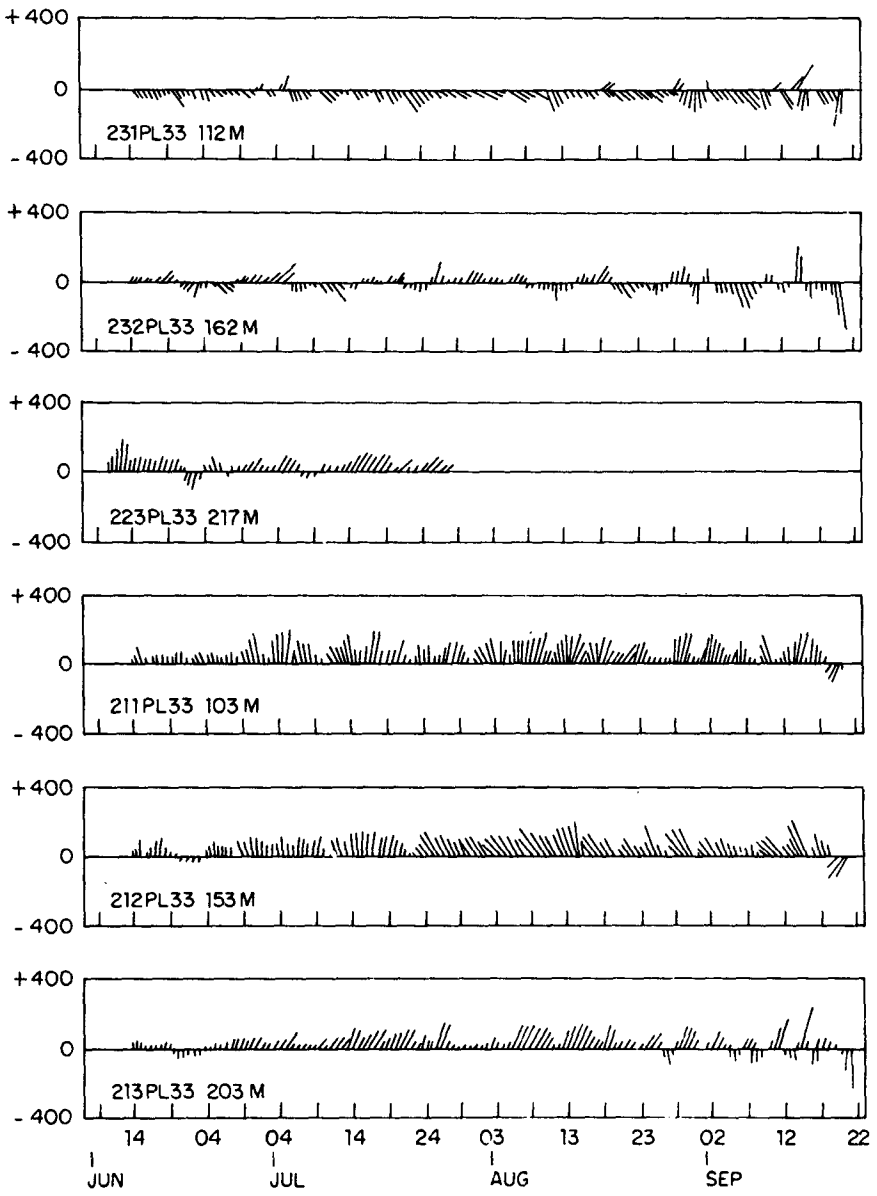

FIG. 4. Stick vector plot of low-passed currents from six different instruments from June through September 1977. The speed scale is in mm s^{-1} and the "up" direction represents in-channel flow.

and current. During both winters, however (Fig. 7), significant coherence existed between axial current and both stress components in the 5–30 day band. For the cross-shore (v) wind stress component, the coherence is greatest in the 4–7 day band with a phase lag not significantly different from 180°, indicating that the offshore wind is associated with inflowing current, and vice versa. For the alongshore (u) wind stress component, the wind leads the current by about 1 day, so that southwest winds are associated with inflowing current, and vice versa. The possible significance of these relationships is investigated in the discussion section.

d. The temperature time series and water mass structure

Plots of the low-passed temperature time series corresponding to the stick vector plots in Figs. 4 and 6 are shown in Figs. 8 and 9, respectively. During summer (Fig. 8) there was a seasonal warming trend of about 1°C per month at the 100-m instruments, which was

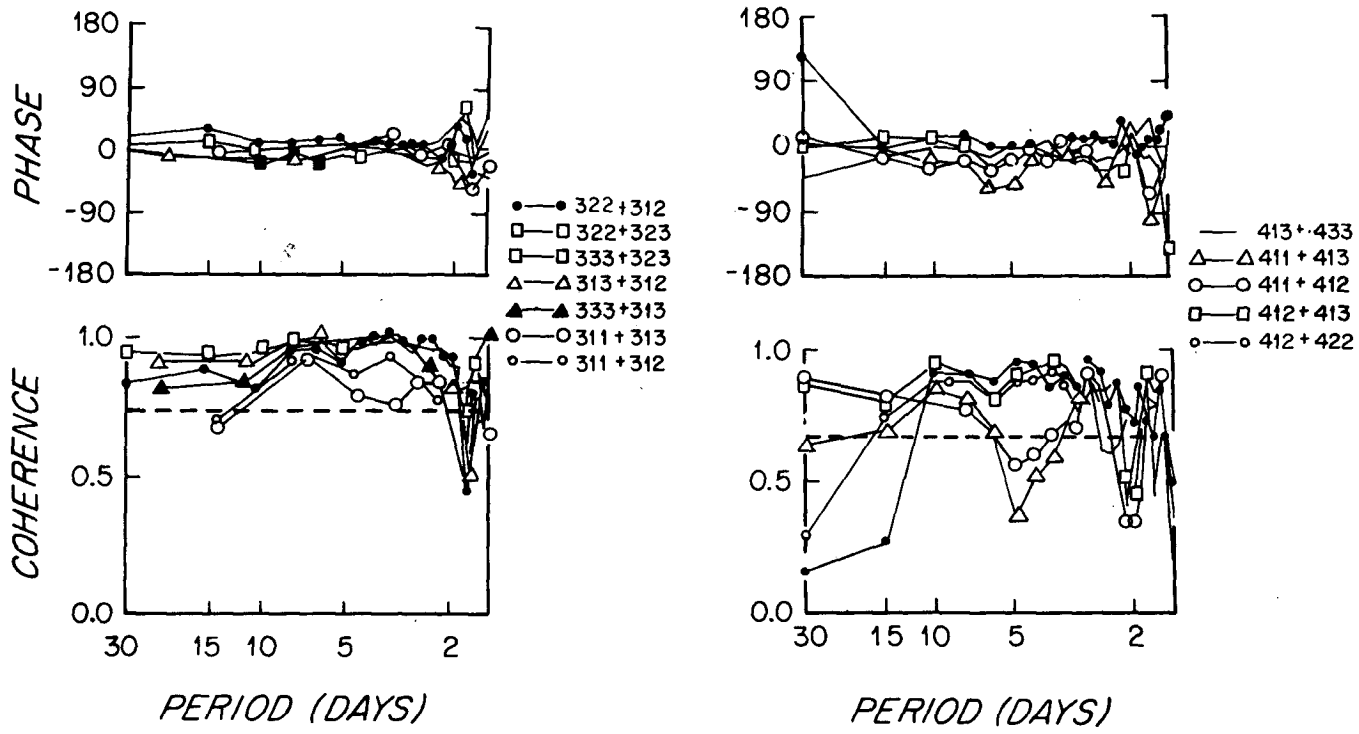

FIG. 5. Low-frequency coherence and phase for axial (v-component) currents measured from September 1977 to March 1978 (left half) and March 1978 to September 1978 (right half). The dashed line on the coherence plot is the 95% significance level.

somewhat reduced at the 150-m instruments and not present near the bottom. Temperatures at mooring 3 (top 3 panels) were quite steady, including instrument 233, which was in the inflow region. The temperature records from moorings 1 and 2 (Fig. 8, bottom 5 panels) were quite different, characterized by large fluctuations with amplitudes from 2 to 5°C, and periods ranging from 4 to 20 days. Figure 9 shows that these fluctuations occurred throughout the year with little seasonal variability. These temperature fluctuations were not well correlated with the bursts of current. Comparing Figs. 4 and 8, for instance, shows that the largest fluctuations at moorings 1 and 2 occurred during a period of very steady channel inflow. Some interannual variability is also evident in the temperature records in Fig. 9. During February–March 1977, temperatures were fairly constant at about 9°C. During this same time period in 1978, temperatures dropped steadily from 10°C to less than 6°C, and remained low throughout the spring.

The water entering Northeast Channel in this 100–220 m depth range comes from similar depths in the Slope Water region between the continental shelf and the north wall of the Gulf Stream. The water masses of this region have been characterized by McLellan (1957), Fuglister (1963), and Gatien (1975, 1976). Two types of Slope Water, the Labrador Slope Water (LSW, T = 6.5–9.0°C, S = 34.25–34.90‰) and the Warm Slope Water (WSW, T = 9.0–12.5°C, S = 35.10–35.50‰) may potentially enter the channel in the 100–200 m depth range. The two water types are separated by the subsurface front whose position is highly variable (Worthington, 1964; Colton, 1968; Gatien, 1975; Horne, 1978), allowing either water type to enter the channel. Hydrographic sections made across the channel can show the presence of either water type (Fig. 10). In Fig. 10a, WSW fills the channel between 100 m and the bottom, whereas in Fig. 10b, LSW occupies this depth range. The range of temperature (6.5–12°C) observed at the current meters moored in the inflow region of Northeast Channel is consistent with the notion that both WSW and LSW enter the channel at different times, and the time scales of the fluctuations suggest that this variability occurs over periods ranging from 4 to 20 days. The outflowing water at mooring 3 consisted of the lower reaches of the Maine Intermediate Water (MIW). This water mass is well mixed within the Gulf of Maine (Hopkins and Garfield, 1979) and therefore shows little variability in temperature when compared with the inflowing water.

4. Transports

a. Volume transport

For the volume transport calculations, the area of the channel below 75 m depth was divided into nine

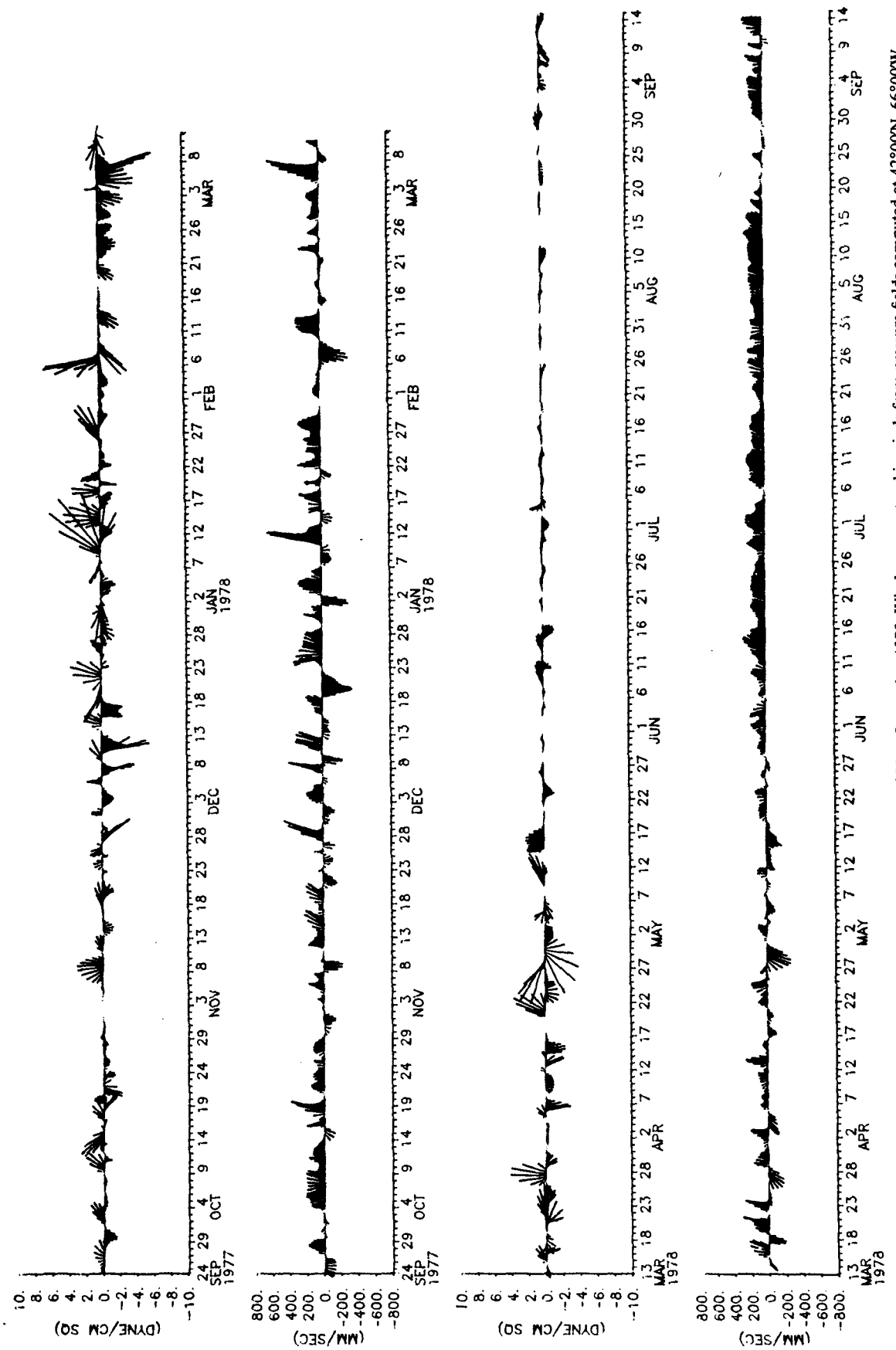

FIG. 6. Wind stress and low-passed current vectors from September 1977 to September 1978. Winds are geostrophic winds from pressure fields computed at 42°00'N, 66°00'W. Currents are from location 12 (150 m depth) and represent the inflow region. In-channel current (onshore wind) is up.

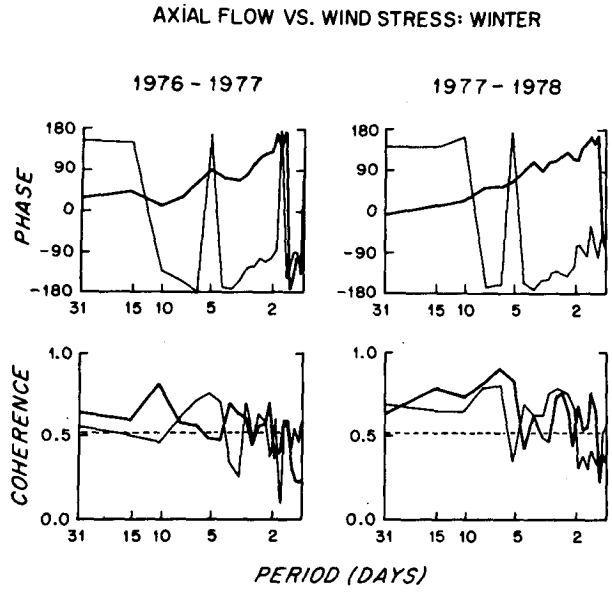

FIG. 7. Coherence and phase between axial current and the alongshore (u—heavy line) and across-shore (v—light line) wind stress components during winter 1976–77 and 1977–78. The dashed horizontal line is the 95% significance level.

boxes with a current meter centered in each box (Fig. 11). The 75 m depth was chosen as the upper limit since it represents the bottom of the seasonal thermocline and the upper limit of the Slope Water intrusions. The velocity data were averaged over 2-week intervals to allow the analysis of the seasonal variation in the volume transport. Biweekly transports were found for each box by multiplying the area of each box by the velocity component normal to the box. The transports in the individual boxes were then summed to obtain the total net transport for that period. Gaps in the record for individual boxes were filled by taking advantage of the very high coherence between certain pairs of instruments mentioned earlier. If an instrument failed at a given location during any one deployment, then data from that location during the other three deployments were correlated with data from adjacent positions to determine how best to estimate the missing values. Overall shear in the water column was also considered, and small adjustments in the magnitude of the interpolated estimates were made to match the overall velocity profile. No effort was made to interpolate across the gap of two-and-one-half months in spring of 1977 when no instruments were in the water. Transport values obtained for the entire channel for each two-week period using these techniques are displayed in Fig. 12. There are three different flow regimes:

1) During summer months there is a steady net transport into the Gulf of Maine averaging about 350 $\times 10^3$ m^3 s^{-1} (0.35 Sv).

2) During winter months the transport varies dramatically from -25 to $+700$ ($\times 10^3$ m^3 s^{-1}) calculated at two-week intervals, but the mean transport for these months is also into the Gulf of Maine at about 260 $\times 10^3$ m^3 s^{-1} (0.26 Sv).

3) During the spring of 1978, April to early June, inflow was at a minimum with some significant outflow. Available data from March to early April 1977 also show reduced transport, prior to the gap until early June.

The mean value of the 46 transport estimates shown in Fig. 12 is 262 $\times 10^3$ m^3 s^{-1} with a standard deviation of 199 $\times 10^3$ m^3 s^{-1}. Assuming that each biweekly transport estimate is independent, the 95% uncertainty in the mean transport value is given by $t_{0.025}(n-1)(s/\sqrt{n})$, where s is the estimated standard deviation of the biweekly time series containing n data points and $t_{0.025}(n-1)$ is given by the Student t distribution for $n-1$ degrees of freedom. Within this uncertainty, the mean transport into the Gulf of Maine below 75 m depth during the entire experiment was 262 $\pm$ 58 ($\times 10^3$ m^3 s^{-1}). If the volume of the Gulf of Maine below 75 m is taken as 7.45 $\times 10^3$ km^3, then this mean transport results in a replacement/flushing time of 329 days or about 11 $\pm$ 2 months for the deep waters of the Gulf of Maine. This transport is two–three times greater than previous estimates. Brown and Beardsley (1978) calculated a transport of 120 $\times 10^3$ m^3 s^{-1} using a box model which conserved volume and salt. Hopkins and Garfield (1979) estimated a channel transport of 80 $\times 10^3$ m^3 s^{-1} from thermohaline considerations.

A search was made for seasonal variation in the volume transport by fitting the function

$$T(t) = M + \sum_{n=1}^{N} (a_n \sin\sigma_n t + b_n \cos\sigma_n t)$$

where $\sigma_n = 2\pi n/(365\text{ d})$ to the biweekly transport time series using multiple least-squares regression methods (Fofonoff and Bryden, 1975; Butman and Beardsley, 1983; Beardsley *et al.*, 1985). This technique was chosen since it works well with short time series in which gaps may be present, and allows the assignment of confidence limits to the results. For this application the biweekly transport estimates were considered independent giving $46 - 2N - 1$ degrees of freedom. The mean and two pairs of coefficients representing annual and semiannual variation were found to be statistically significant. The resulting coefficients and their confidence limits are shown in Table 3, and the fitted curve is shown as a dotted line in Fig. 12. The annual variation consisted of reduced transport in springtime with higher transport during the rest of the year. There was also a marginally significant variation consisting of a slight reduction in transport in the fall relative to approximately equal transport in midsummer and midwinter. It is emphasized that this technique is used only to describe statistically the data in hand, and may not be used to imply that a similar seasonal variation exists in other years in the Northeast Channel.

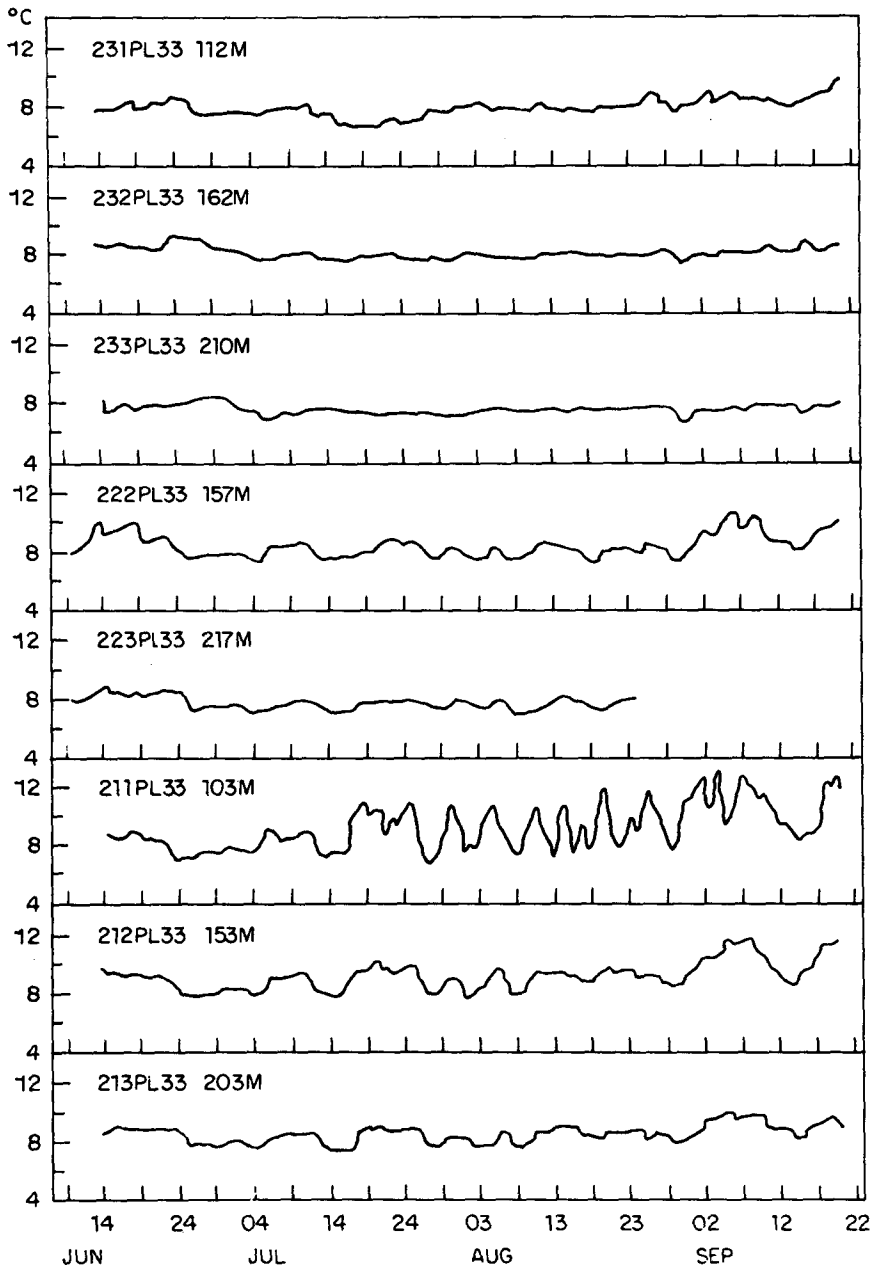

FIG. 8. Low-passed temperature time series from six different instruments from June through September 1977. This temperature plot matches the stick vector plot of Fig. 4.

b. Heat and nitrogen transport

This section focuses on the transport of heat and nitrogen through the channel. An estimate of the salt flux is not included. An attempt was made to create a salinity time series using T–S correlations for the region surrounding the channel, but this series was questionable owing to the overlap in water types between LSW, WSW, and MIW, which prohibited the establishment of a unique T–S relationship.

An accurate heat budget for the Gulf of Maine has not yet been achieved owing to the lack of data at the important boundaries where inflows and outflows occur. The Northeast Channel is one such boundary and data are presented here which will be of use in calculating future heat budgets for the region. Only the second year's data (September 1977–September 1978) have been used for the heat calculations since instrument performance was superior during that time and little interpolation was needed to fill gaps in the data.

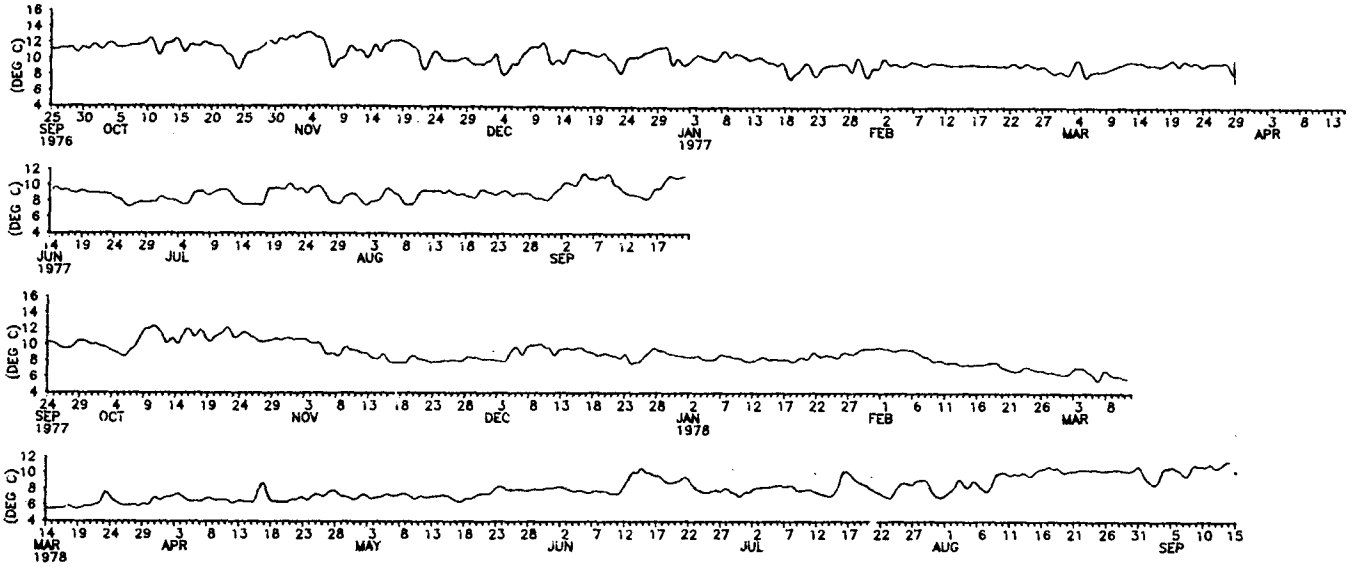

FIG. 9. Low-passed temperature time series from location 12 for September 1976–September 1978. The bottom 2 panels correspond to the stick vector plots of Fig. 6.

The eddy heat flux (Q_e) was calculated for each box in Fig. 11 using the covariance between velocity and temperature:

$$Q_e = \rho C_p \overline{V'T'} A$$

where

- ρ density of seawater in g cm^{-3}
- C_p specific heat of seawater at constant pressure in cal/g-°C
- V' $(= V - \bar{V})$ = deviations from the time-averaged current velocity in cm s^{-1}, with V the velocity component normal to the section
- T' $(= T - \bar{T})$ = deviations from the time-averaged temperature in °C
- A area of the box in cm^2

and overbars denote time averages. The contributions from each box were then summed to find the eddy heat flux for the entire channel below 75 m, which was 173 $\times 10^6$ kcal s^{-1}. The positive sign indicates that the eddy heat flux added heat to the Gulf of Maine, i.e., the temporally fluctuating inflows were warmer than average while the outflowing events were colder. A spectral decomposition of the covariance showed that about 60 percent of the eddy heat flux was due to tidal fluctuations and about 40 percent was due to longer-period fluctuations in the 4–10 day band.

The mean volume transport into the Gulf of Maine of 262 ± 58 ($\times 10^3$ m^3 s^{-1}) had a mean temperature of 7.86 ± 0.42°C. The nonzero mass flux makes it impossible to quantitatively assess the importance of this inflow to the Gulf of Maine heat budget without additional data from the other important inflows and outflows to the Gulf of Maine (i.e., around Cape Sable, through Nantucket Shoals, and over Georges Bank). However, Mountain and Jessen (unpublished data) found a mean temperature below 100 m in the Gulf of Maine from 1979 to 1982 of 6.68 ± 0.70°C. If their data are representative of the long-term conditions in the deep waters within the Gulf, then the deep inflow through the Northeast Channel during 1977–78 most likely warmed the deep waters of the Gulf of Maine.

The mean advective nitrogen transport through the channel has been calculated as the product of the seasonal mean transport through the channel and the seasonal mean nitrate (NO_3) content of the Slope Water. Only nitrate was used since quantities of nitrite (NO_2) present in the Slope Water were negligible by comparison. The winter mean values were 7.3 μmol l^{-1} for the NODC data and 15.7 μmol l^{-1} for the EG&G data for an average winter value of 11.5 μmol l^{-1}. The summer mean values were 15.0 μmol l^{-1} for the NODC data and 20.4 μmol l^{-1} for the EG&G data for an average value of 17.7 μmol l^{-1}. Systematic differences in nitrate content between the Slope Water masses (LSW and WSW) did not exist, and a single average value was used to represent both water types. These data agree closely with those of Pastuszak *et al.* (1982), who determined an annual mean nitrate concentration of 16.4 μmol l^{-1} from data collected in the Slope Water between 120 to 300 m depth along the southern side of Georges Bank. These average values were multiplied by the seasonal mean volume transports to estimate a mean advective nitrogen transport for each of the four arrays. These were then averaged to obtain an annual mean value of 4.05 ± 1.70 ($\times 10^9$ μmol s^{-1}) through the channel (Table 4). Matte *et al.* (1979) suggest that the ammonium concentration in the upper Slope Wa-

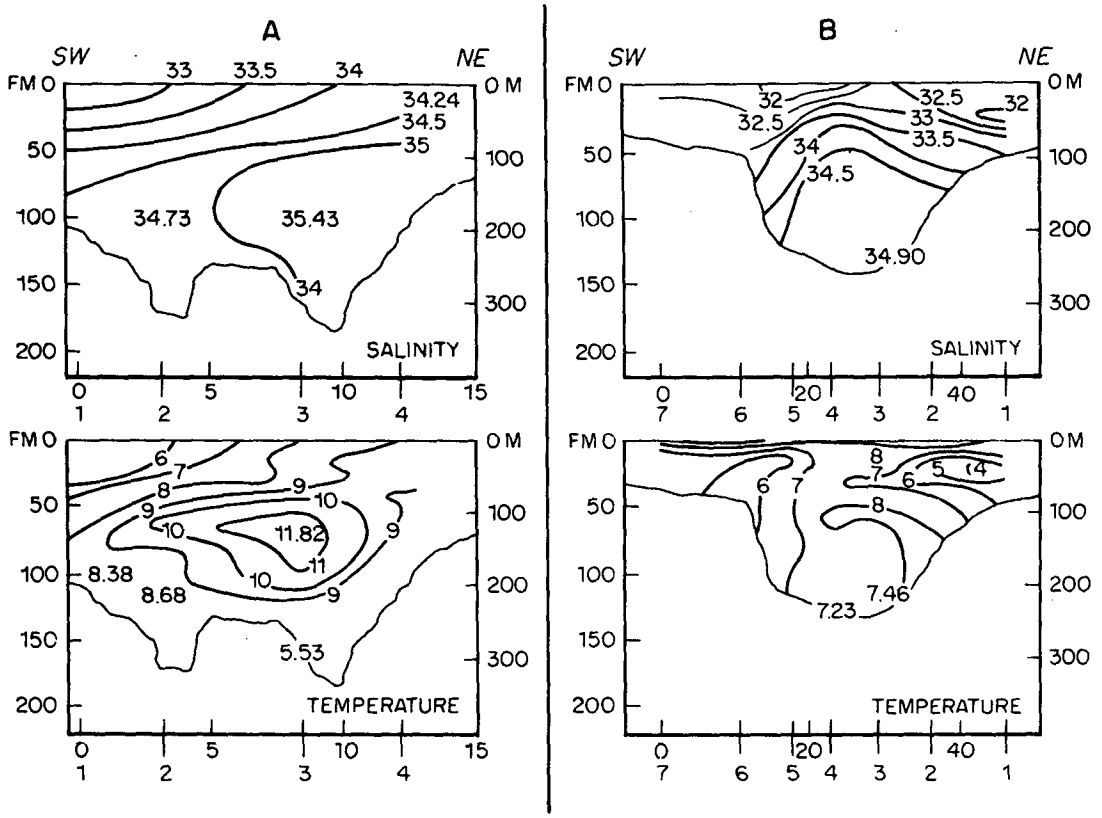

FIG. 10. (a) Hydrographic section across the Northeast Channel (7 May 1975) when a parcel of Warm Slope Water was present; (b) a second hydrographic section (21 May 1975) across the channel when Warm Slope Water was not present.

ter may be as high as 45% of the nitrate concentration. In this case, an additional 1.82×10^9 μmol s^{-1} would be advected through the channel in the form of ammonium, or 5.87×10^9 μmol s^{-1} total. This represents about 33% of the nitrogen demand (17.70×10^9 μmol s^{-1}) estimated by Schlitz and Cohen (1984) for the Gulf of Maine and Georges Bank region.

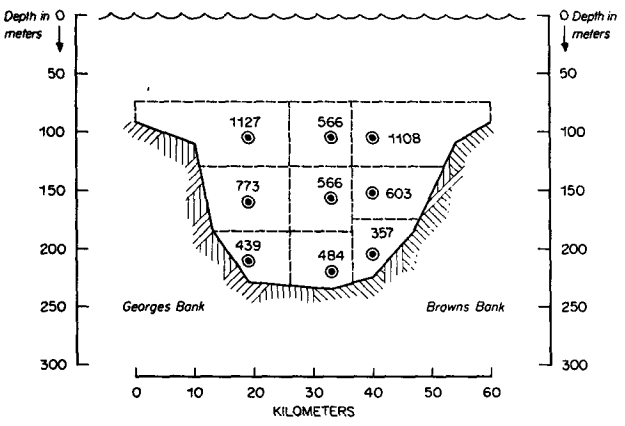

FIG. 11. The cross-sectional areas assigned to each current meter for the transport calculations. The number in each box is its area $\times 10^{-3}$ m^2.

5. Discussion

a. *Wind, pressure, and current*

Atmospheric pressure and sea level data from January through September 1978 were obtained for the Gulf of Maine region from Wendell Brown, University of New Hampshire. The synthetic subsurface pressure (SSP) was calculated from the data at Boston, Massachusetts, Portland and Bar Harbor, Maine, and Yarmouth, Nova Scotia (Fig. 1). The SSP is the algebraic sum of the coastal sea level fluctuations (expressed in pressure-equivalent units) and the atmospheric pressure, and may be used as a proxy for direct bottom pressure measurements (Brown *et al.*, 1984). A single direct bottom-pressure measurement was also obtained from station M_1 (Fig. 1; 42°N, 68°W, 200 m depth) on the north side of Georges Bank (EG&G, 1979b,c,d, 1980). All the pressure time series had the mean removed and were low-pass filtered with the same filter used on the wind and current data. Pressure differences across the Gulf of Maine were also computed. The east–west gradient was approximated by the SSP at Boston minus the SSP at Yarmouth, and the north–south gradient was approximated by the SSP at Portland minus the bottom pressure at M_1.

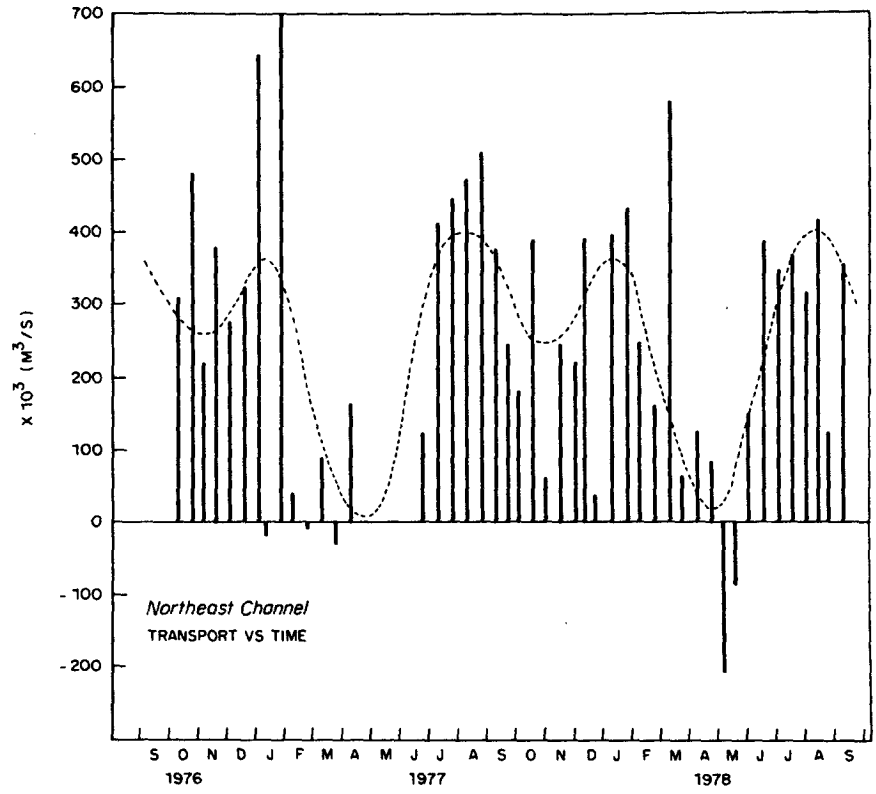

FIG. 12. Bar graph of total transport through the Northeast Channel below 75 m vs time. Each bar represents a two-week average. There were no instruments in the water during the gap in spring of 1977. Negative values represent out-channel flow. The best seasonal fit to the data in the multiple least-squares sense (see text) is indicated as a dotted line.

The SSP field in the western Gulf of Maine was found to be almost totally coherent, as described by earlier investigators (Noble and Butman, 1979; Vermersch *et al.*, 1979; and Brown and Pettigrew, 1984). Using this result, the SSP at Portland was chosen as representative of the coastal SSP field for comparisons with the wind stress and currents measured at Northeast Channel.

The pressure and Northeast Channel time series overlapped only for the January–September 1978 time period, which included only three winter months, January–March 1978. The wind stress components, SSP at Portland, axial current at instrument 412 (northeast side, 150 m depth), and the pressure difference time series are plotted together in Fig. 13 for comparison. The major peaks for all six series were well correlated visually, with the strongest correlation between SSP and current, which were nearly mirror images of each other. The one exception was a large inflow event on 10–15 February that did not appear to be correlated with any of the other series. The autospectra for these series are shown in Fig. 14. Current, SSP, and alongshore wind stress had coincident spectral peaks at a period of 5.6 d. The cross-shore wind and north–south difference spectra peaked at a slightly shorter period

TABLE 3. Results of multiple regression fit of a seasonal model to the biweekly transport estimates. Those coefficients statistically different from zero at 95% confidence are marked with an asterisk.

	Regression coefficients for transport estimates ($\times 10^3$ m^3 s^{-1})
M	246 ± 53
$*a_1$	−123 ± 75
b_1	18 ± 72
$*a_2$	80 ± 75
$*b_2$	83 ± 72

TABLE 4. The transport of volume and nitrate–nitrogen through the Northeast Channel for each of the four six-month arrays.

Array number	Transport ($\times 10^3$ m^3 s^{-1})	Mean NO_3 μmol l^{-1}	N Transport ($\times 10^9$ μmol s^{-1})
1	255	11.5	2.93
2	372	17.7	6.58
3	284	11.5	3.27
4	192	17.7	3.40
Mean			4.05 ± 1.70

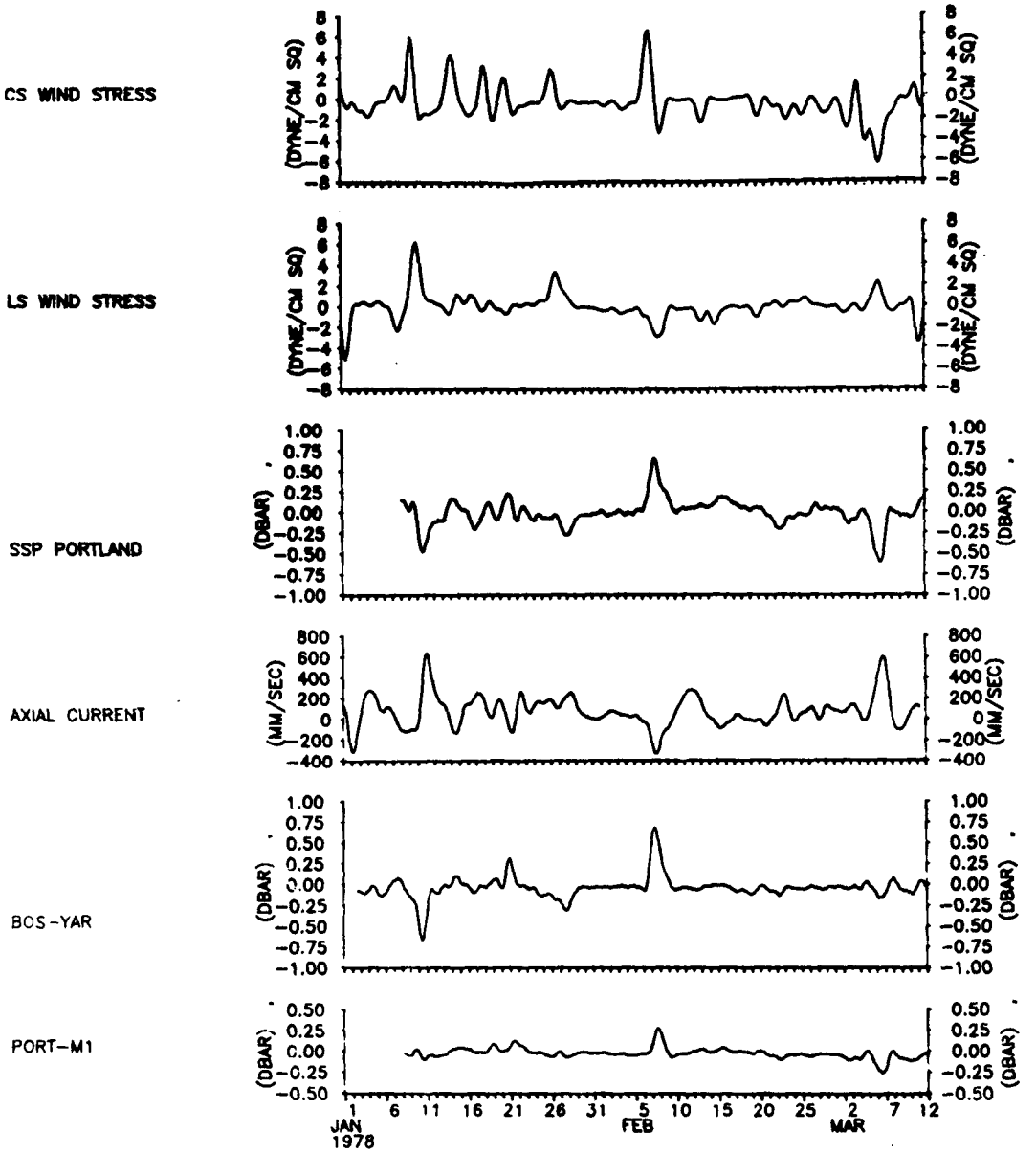

FIG. 13. Time series plots of cross-shore wind stress (positive onshore), alongshore wind stress (positive northeast), SSP Portland, axial current at location 12, east-west pressure differences (Boston–Yarmouth) and north–south pressure differences (Portland–M_1) for the January–March 1978 time period.

(4.5 d) and the east-west differences a bit longer (7.5 d). The coherence and phase between chosen pairs of series (Fig. 15) all show significant low-frequency coherence. Current and SSP were coherent over the entire 2–22 day range, except for one point at 3.75 days which was a spectral valley in both time series. The phase lag in the 4.5–11 day range was not significantly different from 180 degrees, meaning that inflowing currents were associated with drops in coastal SSP and vice versa. The SSP was coherent with alongshore (u) winds at 5.6–22 day periods, but only at 5.6 days with the across-shore wind, with phasing such that drops in SSP were associated with southwest and offshore winds. The wind–current relations for this time were the same as those described earlier using the full six-month time series for both winters, i.e., inflowing currents were associated with offshore and southwest winds, and vice versa. Axial current was coherent with pressure differences at 7–22 day periods with phasing such that positive (inflowing) current was associated with negative differences (Portland–M1 and Boston–Yarmouth) in both the north–south and east–west time series.

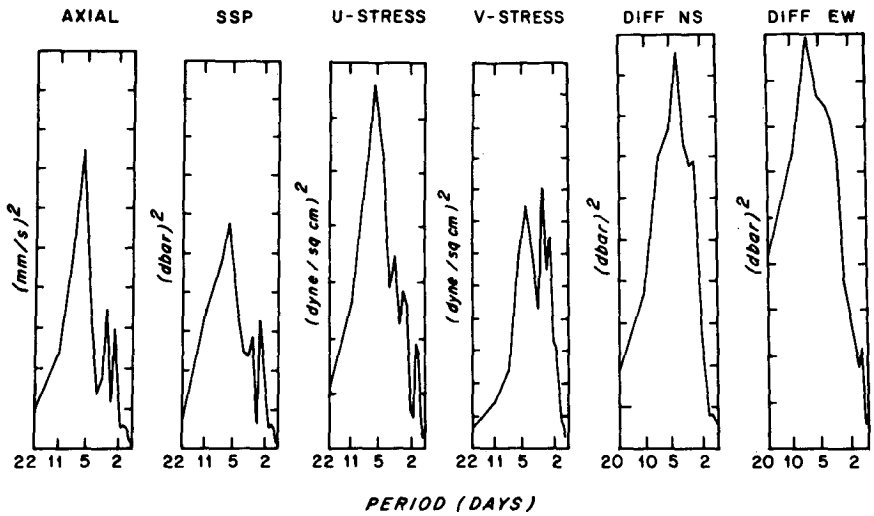

FIG. 14. Variance-conserving autospectra for each of the time series shown in Fig. 13.

During the April–September 1978 time period (not shown), the axial current and SSP time series remained strongly coherent at all periods ranging from 2 to 30 days. This is in marked contrast to the wind stress series which were not coherent with current during the summer months. Another important seasonal difference in SSP and current is that from mid-May to mid-August, the current fluctuations at 2–30 day time scales were small compared to a mean channel inflow of order 20 cm s^{-1}. This mean inflow was not correlated with a long-term set down of coastal SSP that was near zero during this time.

These observations of wind, SSP, and current in Northeast Channel are consistent with a conceptual model in which the current fluctuations in the wind-forced (2–11 day) frequency band are driven by external (barotropic) pressure gradients across the channel sill which are due to the setup and setdown of the Gulf of Maine by the wind stress. Onshore winds and alongshore winds from the northeast create a pressure head

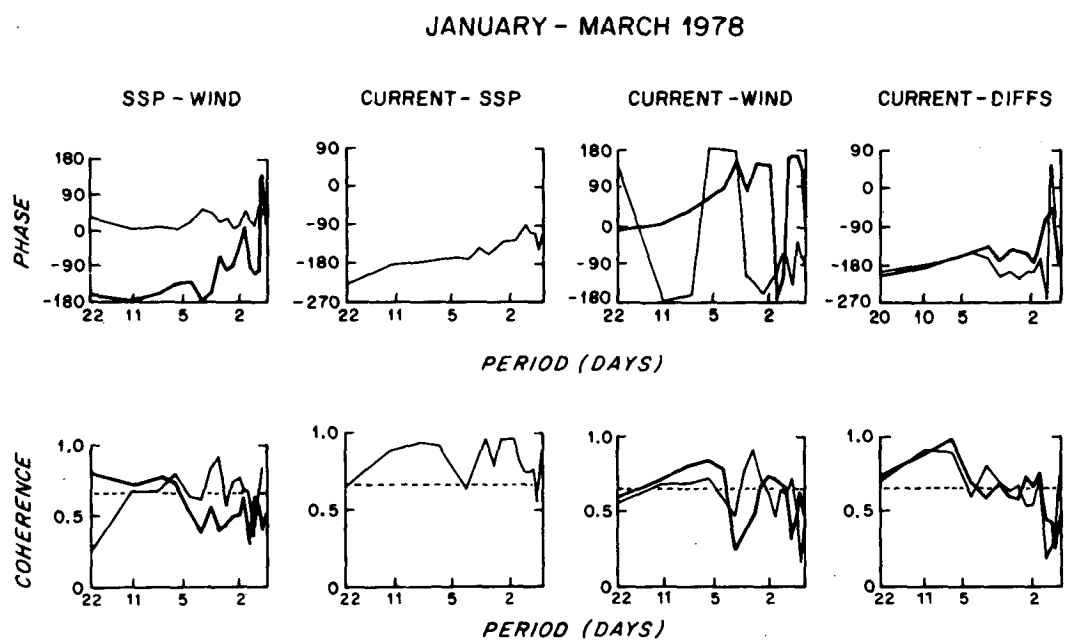

FIG. 15. Coherence and phase plots for pairs of variables plotted in Fig. 13. For pairs involving wind, the heavy line is the alongshore (u) stress component and the thin line is the across-shore (v) stress component. The coherence between current and east–west differences is represented as a heavy line and north–south differences as a thin line. The dashed horizontal line on the coherence plots is the 90% significance level. A positive phase indicates that the first series lags the second by the amount shown.

within the Gulf which is detrimental to channel inflow, while opposing winds have the opposite effect. The data of Table 5 are consistent with this model and summarize the phase relationships for the predominant 5.6-day period. The SSP response lagged alongshore wind stress by 17.6 hours and across-shore wind stress by near 0 hours, consistent with the results of earlier investigators (Noble and Butman, 1979; Vermersch *et al.*, 1979; Brown and Pettigrew, 1984). Once the pressure field had been established, the current response was rapid (approximately 3.7 hours).

Certain seasonal aspects of the channel flow such as the reduced transport in spring and the strong steady inflow in summer are not explained by the above model, and are believed instead to be associated with changes in the internal (baroclinic) pressure gradients across the sill. A mean inflow with a low in the springtime due to the internal pressure field combined with a fluctuating flow of varying strength in the 4–11 day band due to the external pressure field could explain most observed features of the Northeast Channel flow.

b. *Gulf Stream forcing*

A source of channel variability that has not yet been considered is the water movement associated with large Gulf Stream meanders and warm core rings (WCRs). Weekly charts showing the position of these features (Atlantic Environmental Group, Narragansett, Rhode Island) have been closely examined for evidence of any correlation between the positions of meanders and/or WCRs and variations in the current and/or temperature fields in the Northeast Channel.

The only close approach of a Gulf Stream feature to Northeast Channel in the ring data base for the 1976–78 time period was the passage of WCR 77D (Mizenko and Chamberlin, 1978). Between 2 and 22 August 1977, the ring 77D moved straight at the channel mouth at a rate of about 4.6 km day^{-1}, and stopped when its northern edge shoaled on the continental slope directly off the mouth of the channel. The observed channel currents and temperatures during this time (Figs. 4 and 9) were not affected by the ring, which was apparently constrained by its depth, width, and rotational rigidity from ever reaching the channel sill where the current meters were located. This same result was true of all other Gulf Stream meanders and WCRs that were studied, and it is concluded that Gulf Stream features did not play an important role in driving the currents through Northeast Channel.

TABLE 5. Coherence and phase relationships between wind-stress components, coastal SSP, and axial current in Northeast Channel at the dominant 5.6-day period. The 95% significance level is indicated following the coherence. The phase is the time in hours required for the current (SSP) to respond to the forcing. An S or NS following the phase indicates whether the phase value is or is not significantly different from zero.

	Alongshore wind		Cross-shore wind	
	Coh/Sig	Phase	Coh/Sig	Phase
Wind-current	0.93/0.53	21.2 (S)	0.80/0.53	7.2 (NS)
Wind-SSP	0.73/0.73	17.6 (S)	0.79/0.73	1.1 (NS)
SSP-current	0.92/0.73	3.7 (NS)	0.92/0.73	3.7 (NS)

6. Summary

Moored current and temperature data have been obtained from below 100 m depth in the Northeast Channel from September 1976 to September 1978. The mean flow consisted of an outflow at the 100 and 150 m depths on the southwest side of the channel and an inflow everywhere else. Mean speeds ranged from 2.1 to 7.0 cm s^{-1} in the outflow region and 3.3 to 10.1 cm s^{-1} in the inflow region. The temperature time series and associated hydrographic sections suggest that the outflowing water was mostly Maine Intermediate Water while the inflowing water consisted of both Warm Slope Water and Laborardor Slope Water. Low-frequency motions varied seasonally in character. During winter, strong bursts of current with periods ranging from 4 to 11 days and magnitudes of up to 60 cm s^{-1} flowed into and out of the channel. During summer, much smaller fluctuations were imbedded on a larger steady flow of about 20 cm s^{-1}. Correlations between the observed low-frequency currents, the surface wind stress, and coastal SSP are consistent with a model in which the current fluctuations are driven by external (barotropic) pressure gradients set up by the wind stress over the Gulf of Maine. Additional field work and modeling efforts are needed to confirm the suggested relationships.

The mean and seasonal variation in the volume transport of the deep flow was computed from a time series of 46 biweekly transport estimates. The mean transport was into the Gulf of Maine at 262 ± 58 ($\times 10^3$ m^3 s^{-1}). A multiple least-squares fit to the transport series showed a strong, significant reduction in transport in the spring, and a weak, marginally significant reduction in the fall. The heat transport through the channel could be only partially determined, since the mass flux through the channel was not locally balanced. The eddy heat flux added heat to the Gulf of Maine at a rate of 173×10^6 kcal s^{-1}. The nitrogen flux added at least 4.05×10^9 μmol s^{-1} to the Gulf of Maine, and possibly as much as 5.87×10^9 μmol s^{-1} if the ammonium contribution were included.

Acknowledgments. The authors are indebted to J. Vermersch and R. Beardsley of the Woods Hole Oceanographic Institution (WHOI) for assistance with the initial mooring design, deployment, and data processing for the first six months of the experiment. Derek Sutton (NMFS) did much of the subsequent computer processing and graphical display. David Mountain (NMFS) and Robert Beardsley (WHOI) provided helpful scientific advice. John Moody (USGS) performed the tidal harmonic analysis. David Chapman (WHOI) performed the seasonal least-squares fit to the

transport data. The coastal sea level and atmospheric pressure data was generously provided by Wendell Brown of the University of New Hampshire. Two anonymous referees made very helpful comments on an earlier version of the manuscript. We thank the officers and crew of the NOAA ships R.V. *Albatross IV* and *Mt. Mitchell,* and the tug *Whitefoot,* for their assistance in the deployment and recovery of the moorings at sea. Cheryl Windsor patiently and professionally typed several versions of the manuscript. These measurements were carried out as part of the Marine Resources Monitoring, Assessment, and Prediction (MARMAP) Program of the U.S. National Marine Fisheries Service.

REFERENCES

Beardsley, R. L., D. C. Chapman, K. H. Brink, S. R. Ramp and R. J. Schlitz, 1985: The Nantucket Shoals Flux Experiment (NSFE79). Part 1: A Basic description of the current and temperature variability. *J. Phys. Oceanogr.,* **15,** 713–748.

Bigelow, H. B., 1927: Physical oceanography of the Gulf of Maine. *Bull. Bur. Fish.,* **40**(Part II), 511–1027.

Brown, W. S., 1984: A comparison of Georges Bank, Gulf of Maine and New England shelf tidal dynamics. *J. Phys. Oceanogr.,* **14,** 145–167.

——, and R. C. Beardsley, 1978: Winter circulation in the western Gulf of Maine. Part I: Cooling and water mass formation. *J. Phys. Oceanogr.,* **8,** 267–277.

——, and N. R. Pettigrew, 1984: Subtidal pressure variability in the Gulf of Maine and on the adjacent shelf. Unpublished manuscript.

——, —— and J. Irish, 1984: The Nantucket Shoals Flux Experiment (NSFE79). Part II: The structure and variability of across-shelf pressure gradients. *J. Phys. Oceanogr.,* **15,** 749–771.

Bumpus, D. F., 1973: A description of the circulation on the continental shelf of the east coast of the United States. *Progress in Oceanography,* Vol. 6, Pergamon, 11–157.

——, 1976: Review of the physical oceanography of Georges Bank. *Int. Comm. Northwest Atl. Fish. Res. Bull.,* **12,** 119–134.

Butman, B., and R. C. Beardsley, 1983: Long-term observations on the southern flank of Georges Bank: Seasonal cycle of currents and temperature. *J. Phys. Oceanogr.,* (submitted).

Colton, J. B., Jr., 1968: Recent trends in subsurface temperatures in the Gulf of Maine and contiguous waters. *J. Fish. Res. Bd. Can.,* **25,** 2427–2437.

——, 1969: Temperature conditions in the Gulf of Maine and adjacent waters during 1968. *J. Fish. Res. Bd. Can.,* **26,** 2746–2751.

Dennis, R. E., and E. E. Long, 1971: A users guide to a computer program for harmonic analysis of data at tidal frequencies. NOAA Tech. Rep. NOS41, 29 pp.

EG&G Environmental Consultants, 1978: Data Report, Nutrients data September 1977 and November 1977, Appendix E, Seventh Quarterly Progress Report, New England Outer Continental Shelf Physical Oceanography Program, Waltham, MA, 17 pp.

——, 1979a: Data Report, Plankton-Nutrients studies December 1978, Appendix C, 10th Quarterly Progress Report, New England Outer Continental Shelf Physical Oceanography Program, Waltham, MA, 49 pp.

——, 1979b: Data Report, Eulerian studies, January 1978–February 1979, Appendix B of the Tenth Quarterly Progress Report. New England Outer Continental Shelf Physical Oceanography Program. EG&G Environmental Consultants, Waltham, MA, 79 pp.

——, 1979c: Data Report, Eulerian studies, April 1978–May 1979, Appendix B of the Eleventh Quarterly Progress Report. New England Outer Continental Shelf Physical Oceanography Program. EG&G Environmental Consultants, Waltham, MA, 111 pp.

——, 1979d: Data Report, Eulerian studies, March 1979–August 1979, Appendix B of the Twelfth Quarterly Progress Report. New England Outer Continental Shelf Physical Oceanography Program. EG&G Environmental Consultants, Waltham, MA, 107 pp.

——, 1980: Data Report, Eulerian studies, November 1979–January 1980, Appendix B of the Thirteenth Quarterly Progress Report. New England Outer Continental Shelf Physical Oceanography Program. EG&G Environmental Consultants, Waltham, MA, 77 pp.

Flagg, C. N., J. A. Vermersch and R. C. Beardsley, 1976: 1974 M.I.T. New England Shelf Dynamics Experiment (March 1974), Data Report. Part II: The Moored Array. M.I.T. Tech. Rep. 76-1, 22 pp.

Fofonoff, N. P., and H. Bryden, 1975: Specific gravity and density of seawater at atmospheric pressure. *J. Mar. Res.,* **33**(Suppl.), 69–82.

Fuglister, F. C., 1963: Gulf Stream '60. *Progress in Oceanography,* Vol. 1, Pergamon, 365–373.

Gatien, M. G., 1975: A study in the slope water region south of Halifax. M.S. thesis, Dalhousie University, Halifax, N.S., 134 pp.

——, 1976: A study in the slope water region south of Halifax. *J. Fish. Res. Bd. Can.,* **33,** 2213–2217.

Hopkins, T. S., and N. Garfield, III, 1979: Gulf of Maine intermediate water. *J. Mar. Res.,* **37,** 103–139.

Horne, E. P. W., 1978: Interleaving at the subsurface front in the slope water off Nova Scotia. *J. Geophys. Res.,* **83,** 3659–3671.

Lauzier, L. M., 1967: Bottom residual drift on the continental shelf area of the Canadian Atlantic coast. *J. Fish. Bd. Can.,* **24,** 1845–1859.

Matte, A., R. Waldhauer and D. A. F. Draxler, 1979: Nutrient data from cruise of the Whiting FRC 05-06, 29–31 May 1979. Laboratory Rep. SHL 79-39, NMFS, NEFC, Sandy Hook Laboratory, 17 pp.

McLellan, H. J., 1957: On the distinctness and origin of the slope water off the Scotian Shelf and its easterly flow south of the Grand Banks. *J. Fish. Res. Bd. Can.,* **14,** 213–239.

Mizenko, D., and J. L. Chamberlin, 1978: Gulf Stream anticyclonic eddies (Warm Core Rings) off the northeastern United States in 1977. *Ann. Biol.,* **34,** 39–44.

Moody, J. A., B. Butman, R. C. Beardsley, W. S. Brown, P. Daifuku, J. D. Irish, D. A. Mayer, H. O. Mofjeld, B. Petrie, S. Ramp, P. Smith and W. R. Wright, 1984: Atlas of tidal elevations and current observations on the northeast American continental shelf and slope. USGS Bull. No. 1611, 122 pp.

Noble, M., and B. Butman, 1979: Low-frequency wind-induced sea level oscillations along the east coast of North America. *J. Geophys. Res.,* **84,** 3227–3236.

Pastuszak, M., W. R. Wright and D. Patanjo, 1982: One year of nutrient distribution in the Georges Bank region in relation to hydrography, 1975–1976. *J. Mar. Res.* **40**(Suppl), 525–542.

Pawlowski, R. J., 1977: A description of the hydrographic characteristics and water masses of the Northeast Channel, Gulf of Maine. Unpublished manuscript, Northeast Fisheries Center, Woods Hole, MA, 22 pp.

Schlitz, R., and E. Cohen, 1984: A nitrogen budget for the Gulf of Maine and Georges Bank. *Biol. Oceanogr.,* **3,** 203–221.

Tee, K-T., 1979: The structure of three-dimensional tide generating currents. Part I: Oscillating Currents. *J. Phys. Oceanogr.,* **14,** 145–167.

Vermersch, J. A., R. C. Beardsley and W. S. Brown, 1979: Winter circulation in the western Gulf of Maine. Part 2: Current and Pressure Observations. *J. Phys. Oceanogr.,* **9,** 768–784.

Worthington, L. V., 1964: Anomalous conditions in the slope water area in 1959. *J. Fish. Res. Bd. Can.,* **21,** 327–333.

Wright, W. R., 1979: High salinity in the Georges Bank region in February 1977. *Ann. Biol.,* **34,** 34–36.